Cofactor Regeneration of NAD^+ from NADH: Novel Water-Forming NADH Oxidases

Bettina R. Riebel,[a] Phillip R. Gibbs,[b] William B. Wellborn,[b] Andreas S. Bommarius[b,*]

[a] Department of Pathology, Whitehead Building, 615 Michael Drive, Emory University, Atlanta, GA, 30322, USA
[b] School of Chemical Engineering, Georgia Institute of Technology, 315 Ferst Drive, Atlanta, GA 30332-0363, USA
Fax: (+1)-404-894-2291, e-mail: andreas.bommarius@che.gatech.edu

Received: August 7, 2002; Accepted: September 19, 2002

This work is dedicated to Roger A. Sheldon, a trusted colleague and friend as well as a leader in the field of biocatalysis, upon the occasion of his 60th birthday.

Abstract: Dehydrogenases with their superb enantioselectivity can be employed advantageously to prepare enantiomerically pure alcohols, hydroxy acids, and amino acids. For economic syntheses, however, the co-substrate of dehydrogenases, the NAD(P)(H) cofactor, has to be regenerated. Whereas the problem of regenerating NADH from NAD^+ can be considered solved, the inverse problem of regenerating NAD^+ from NADH still awaits a definitive and practical solution. A possible solution is the oxidation of NADH to NAD^+ with concomitant reduction of oxygen catalyzed by NADH oxidase (E.C. 1.6.-.-) which can reduce O_2 either to undesirable H_2O_2 or to innocuous H_2O. We have found and cloned two novel genes from *Borrelia burgdorferi* and *Lactobacillus sanfranciscensis* with hitherto only machine-annotated NADH oxidase function. We have overexpressed the corresponding proteins and could prove the annotated function to be correct. As demonstrated with a more sensitive assay than employed previously, the two novel NADH oxidases reduce O_2 to H_2O.

Keywords: cofactor; cofactor regeneration; enzymes; NADH oxidase; redox chemistry

Introduction and Motivation

Regeneration of Nicotinamide-Containing (NAD(P)(H)) Cofactors

Enantiomerically pure compounds (EPCs), especially amino and hydroxy acids as well as alcohols, amines, and lactones are increasingly useful in the pharmaceutical, food, and crop protection industries as building blocks for novel compounds not accessible through fermentation[1–4] as well as for asymmetric synthesis templates.[5–6] One very advantageous route to a wide variety of EPCs is the use of dehydrogenases, to afford either reduction of keto compounds or oxidation of alcohol or amine groups. The repertoire of dehydrogenases useful for synthesis of EPCs encompasses alcohol dehydrogenases (ADHs),[7] D- and L-lactate dehydrogenases (LDHs),[8] D- or L-hydroxyisocaproate dehydrogenases (D- or L-HicDHs),[9,10] or amino acid dehydrogenases such as leucine dehydrogenase (LeuDH),[10] phenylalanine dehydrogenase (PheDH)[11–13] or glutamate dehydrogenase (GluDH).[14] Monooxygenases have been used to synthesize, regio- and enantioselectively, lactones from cyclic ketones useful in the flavor and fragrance industries.[15]

Dehydrogenases and monooxygenases need nicotinamide-based cofactors, such as NAD^+ and $NADP^+$ or their reduced equivalents, NADH and NADPH, to function. Economic use of dehydrogenases and cofactor necessitates cofactor regeneration.[16]

For reductive reactions with dehydrogenases or for monooxygenases, NAD(P)H has to be regenerated from $NAD(P)^+$. For this problem, the system formate dehydrogenase (FDH)/formate is now used almost universally (for reviews, see refs.[17–19]). FDH catalyzes the oxidation of inexpensive and easily available formate to carbon dioxide while simultaneously reducing the biological cofactor NAD^+ to NADH (Equation 1).

$$HCOOH + NAD^+ \longrightarrow NADH + H^+ + CO_2 \quad (1)$$

FDH functions as a universal regeneration enzyme in tandem with dehydrogenases catalyzing extremely enantioselective reduction reactions.[20,21]

For oxidative reactions requiring regeneration of $NAD(P)^+$ from NAD(P)H, no universal cofactor regeneration system is known. Alcohol dehydrogenase (ADH) itself can be utilized to catalyze both the oxidative production reaction as well as the reductive regeneration reaction by adding isopropyl alcohol which

  1615-4150/02/34410-1156 – 1168 $ 17.50-.50/0

is oxidized to acetone, but such a scheme tends to be equilibrium-limited and plagued by deactivation of ADH.[22] Both the ADH and the lactate dehydrogenase (LDH) systems[23] cannot take NADPH, in contrast to glutamate dehydrogenase (GluDH), which has been utilized to reduce α-ketoglutarate to L-glutamate.[24,25] NADH oxidases from thermophiles have been employed which regenerate NAD^+ from NADH by reducing O_2 to H_2O_2.[26] In the present work, we propose the oxidation of NADH to NAD^+ with the concomitant reduction of molecular oxygen to water as a solution to the cofactor regeneration problem from NADH to NAD^+.

NADH Oxidases

NADH oxidases (E.C. 1.6.-.-) catalyze the oxidation of NADH by simultaneously reducing molecular O_2 to either hydrogen peroxide, H_2O_2, in a two-electron reduction (Equation 2), or directly to water in a four-electron reduction (Equation 3).

$$NADH + O_2 + H^+ \longrightarrow NAD+ + H_2O_2 \quad (2)$$

$$2\ NADH + O_2 + 2\ H^+ \longrightarrow 2\ NAD+ + 2\ H_2O \quad (3)$$

NADH oxidases contain a second cofactor, presumably covalently bound FAD, as evidenced by the consensus sequence GXT(H/S)AG near the N-terminus, and are widespread among different, evolutionary distinct organisms, such as humans, vertebrates, plants, *Drosophila* and different strains of bacteria. Bacteria harbor both H_2O_2-forming and H_2O-forming NADH-oxidases. Owing to the deactivation of almost all proteins upon the exposure to H_2O_2, the H_2O-forming enzymes should be vastly superior as biocatalysts. Addition of catalase could potentially destroy H_2O_2 formed, however, catalase itself features a very high K_M value of 1.1 M,[27] so that the enzyme is not particularly active at low H_2O_2 concentrations. Thermophilic bacteria usually only feature peroxide-producing NADH oxidases, which, despite their superior stability, renders them unfavorable for catalytic purposes. Water-producing NADH-oxidases can be found in various organisms, such as *Streptococcus*, *Enterococcus*, *Lactobacillus*, *Mycobacterium*, *Methanococcus*, or *Leuconostoc*. These organisms can contain both water- as well as peroxide-producing enzymes.

Various H_2O-producing NADH-oxidases have been found and described in the literature (see Table 1). None of them, however, has been characterized with respect to all the properties relevant to their use as a biocatalyst. In most cases, kinetic properties have not been reported.

Sequence analysis of the water-producing enzymes in all the organisms listed above reveals the same highly conserved cysteine residue, compared to a rather modest overall sequence similarity. This suggests that all these flavoproteins constitute a distinct class of FAD-dependent oxidoreductases, different from others such as glutathione reductase and thioredoxin reductase. Other properties of the enzymes listed above are similar: the molecular weight of the subunit hovers around 50 kD, all enzymes are dimers and contain 1 FAD per subunit, also, all are inactivated by hydrogen peroxide.

An important question concerns the mechanism by which some NADH oxidases reduce oxygen to water while others reduce oxygen only to hydrogen peroxide. Important mechanistic knowledge about NADH oxidase was gleaned from structural elucidation of a closely related enzyme, NADH peroxidase: the crystal structure of NADH peroxidase from *Enterococcus faecalis* suggested a novel mechanism for peroxidases without a heme or metal group. A catalytic cysteine cycles between two distinct states, a thiolate anion and a sulfenic acid.[36] The following year, Ross and Claiborne argued on the first well characterized NADH oxidase, also from *Enterococcus faecalis*, featuring 44% sequence identity to its NADH peroxidase counterpart, that the same novel catalytic mechanism applies for NADH oxidases, involving the same, highly conserved Cys42, which exists as a stabilized sulfenic acid (Cys-SOH) and serves as a non-flavin redox center.[30] This notion was strongly supported by the production of Cys42 mutants which led to production of H_2O_2 instead of water.[37] The primary intermediate is surmised to be a peroxy flavine; the missing Cys42 cannot reduce the peroxy flavine in the subsequent step to produce water.

Table 1. NADH oxidases described so far.

Bacteria	Enzyme	Crystal Structure	Accession Code	Sequence Data	Reference
Leuconostoc mesenteroides	Nox, H_2O				[28]
Enterococcus faecalis	NPX	Mande[34]Yeh[35]	P37062 (SwissProt)	Protein, Nucleotide	[29]
Enterococcus faecalis	Nox, H_2O		P37061 (SwissProt)	Protein, Nucleotide	[30]
Mycoplasma genitalis	Nox, H_2O		Q49408 (EMBL)	Protein, Nucleotide	[31]
Streptococcus mutans	Nox, H_2O		D49951 (EMBL)	Protein, Nucleotide	[32]
Mycoplasma pneumoniae	Nox, H_2O		P75389 (SwissProt)	Protein, Nucleotide	
Methanococcus japanicus	Nox, H_2O		Q58065 (EMBL)	Protein, Nucleotide	[33]

This would implicate the existence of the same thiolate anion structure, which reduces a peroxide through nucleophilic attack. As of yet, however, there is no crystal structure of NADH oxidase to definitely confirm this reaction mechanism.

This contribution reports the cloning, overexpression, purification, and kinetic data of the two novel water-producing NADH oxidases from *Lactobacillus sanfranciscensis* and *Borrelia burgdorferi*.

Results

Cloning and Overexpression

Gene Isolation and Amplification of nox Coding Sequences

The nox coding genes from *Borrelia burgdorferi* (bnox) and *Lactobacillus sanfranciscensis* (sfnox) were isolated from the genomic DNA using gene specific primers derived from the coding sequence. Amplification in PCR succeeded using the PCR failsafe kit (Epicentre, Madison) to yield products of the predicted size of 1335 bp for bnox and 1356 bp for sfnox in several of the 12 buffers provided with the kit (Figure 1). The primers were designed to contain convenient restriction sites (EcoR1 and HindIII for sfnox and BamH1 + HindIII as well for bnox) at both ends to facilitate the following cloning step.

DNA electrophoresis on a 1% agarose gel demonstrates amplification of the nox genes under different PCR-buffer conditions (Figure 1, lanes A through L). As expected, single bands in each lane was found at around the 1300 bp band for bnox and between 1300 and 1400 bp for the sfnox.

Depending on buffer conditions, strong or weak amplification was observed with both nox genes. Each one of the strongest bands (C for bnox and B,C for sfnox) was cut out of the 1% agarose gel and purified using the gel purification kit (Qiagen, Hilden).

Cloning of the nox Genes

Both gene products as well as the pbluescript vector (Stratagene) were restricted with the following enzymes: bnox with BamH1 and HindIII and sfnox with EcoR1 and HindIII. Following restriction, the genes and the vector were purified through gel electrophoresis and subsequent elution (gel purification kit, Qiagen, Hilden). Both genes were separately cloned into the pbluescript vector (Stratagene, La Jolla) and transformed into the *E. coli* XL1blue strain (Stratagene, La Jolla). Positive clones were screened using colony PCR and restriction analysis.

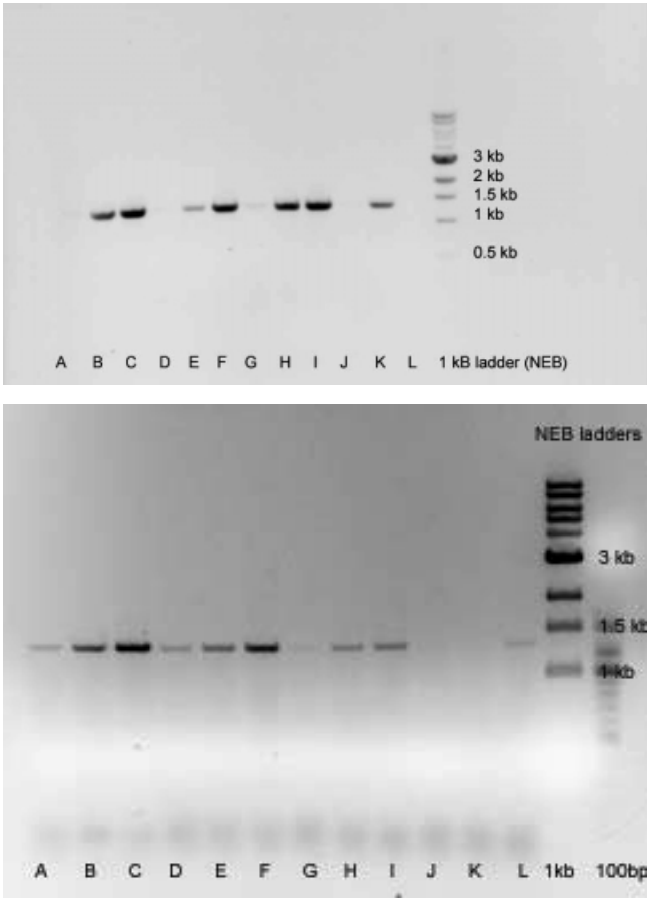

Figure 1. **A**: Amplification of bnox; positive amplification could be achieved using buffers A, B–F, H, I and a weak signal using buffer G, J, and L. No amplification was observed with the buffer K. **B**: Amplification of sfnox; a strong positive amplification could be achieved with buffers B, C, E and F, a weaker signal with A, D, H, I and L. No amplification was achieved with J and K. Compared with bnox, the first round of amplification gave weaker overall signals, so that the PCR band from B and C was cut out of the agarose gel, purified and reamplified in a second PCR reaction using the same conditions and buffers.

Nucleotide Sequence

Nucleotide data corresponding to the 1335 bp of bnox and 1356 bp for sfnox, starting with ATG, were obtained through cycle sequencing using an ABI prism sequencer. Nucleotide sequence and deduced open reading frames are shown in Figure 2. Sequencing templates were the pbluescript-constructs. The open reading frame for both noxes is capable of encoding a protein with a molecular mass of 48.8 kD for sfnox and 48 kD for bnox, which is in good agreement with previously published similar water-producing NADH oxidases. SDS-PAGE of the proteins derived from the expressed genes exhibited a prominent band at around 45 – 50 kD. The GC content of the genes coding for bnox and sfnox

are very low, 32% and 37%, respectively, consistent with the range reported by Ross and Claiborne.[30]

Heterologous Expression in E. coli

The pbluescript constructs were used to cut out the desired gene and subclone it into the expression vector pkk223-3 (Amersham) or pBTac2 (Roche), respectively. With this method no additional PCR was required and risk for additional PCR errors was avoided. Subcloning was successful using the Rapid DNA ligation kit (Roche) and the ligation was transformed into competent HB101 (Stratagene, La Jolla) or M15 *E. coli* strains (Qiagen, Hilden). Colonies formed were tested for successful incorporation through colony PCR.

Two successful clones of each construct were expressed at 37 °C and harvested after 4 h of IPTG induction (sfnoxK2 and sfnoxK6 for *L. sanfranciscensis* and bnoxK1 and bnoxK6 for *B. burgdorferi*). Cell density was equalized to an OD_{600} of 5.0 and then ultrasonicated in 200 μL of 100 mM TEA pH 7.5 buffer. Equal amounts of each fraction, soluble and insoluble, induced and uninduced, were loaded onto a 12.5% SDS-PAGE. Results of the electrophoresis are featured in Figure 4. At 37 °C, the sfnoxK6 clone demonstrates a high level of overexpression in the insoluble fraction, possibly owing to the additional mutation, which could result in lesser stability. BnoxK1 does not show an overexpression, and the expression level of bnoxK6 is slightly lower than that of sfnoxK2. In the case of sfnoxK2, the addition of helper plasmid pREP4 resulted in less uninduced expression when compared to the same clone without the helper plasmid (compare lanes 1 and 2 with 3 and 4).

Sequence Analysis

As already expected from the databases, comparison of the amino acid sequences between sfnox and bnox revealed a rather modest sequence identity of 32%. The consensus sequences were clearly discernible: the FAD-binding site motif GXT(H/S)AG in position 8–14 (counted from the bnox N-terminus), the putative catalytic cysteine residue in position 42, and the NAD-binding site GXGYIG in positions 156–161. Alignment with the sequences of the NADH oxidases of *Enterococcus faecalis*[30] and *Streptococcus mutans*[32] demonstrate at most 34% identity between any two including the two novel proteins, except for 55% between sfnox and the enzyme from *E. faecalis.*

Sequence analysis of both sfnox and bnox genes revealed differences when compared to the annotated nucleotide sequences derived from the NCBI databank (accession files AB035801 for sfnox and NC 001318 for bnox). Both fully sequenced sfnox clones, sfnoxK2 and sfnoxK6, featured a amino acid change from alanine to valine at position 30 (A30V). SfnoxK6 showed an additional change from lysine to arginine at position 102 (K102R). Both constructs, when overexpressed, showed comparable activity. We therefore believe that position 102 does not diminish enzyme activity and that sfnoxK2 with its sequence difference in position 30 shows the correct sequence for an NADH oxidase from *L. sanfranciscensis* rather than the sequence annotated in the databases. In the case of bnox, the two fully sequenced clones revealed several mutations of bnoxK1 and still two, N175S and E221G, in the case of bnoxK6. The latter mutations, however, are not found in bnoxK1 so that we cannot present a wild-type protein in this case. As significant catalytic activity is found on bnoxK6, the mutations do not seem to inhibit activity *per se*. Since we cannot predict the level of activity in the wild-type, no purification scheme on this enzyme was performed until the correct sequence will be elucidated.

Biochemical Characterization

Purification of NADH Oxidases

The purification table for sfnoxK2 is shown in Table 2, with a corresponding gel shown in Figure 5. The procedure results in a strong single prominent band at 50 kDa in the protein gel analysis, is scaleable, and results in high yields. Acid precipitation as the first resolution eliminates buffer/salt exchanges and leaves the final protein preparation in stabilizing levels of ammonium sulfate.[38] Due to the lower loading capacity of the Mono-Q column only 2 mL of the acid-precipitated lysate were loaded and therefore the overall yield was estimated by scaling the subsequent yields by a factor of 5.25 (10.5 mL/2 mL).

Employing the same purification steps but in a different sequence [lysate – 45% ammonium sulfate precipitation – acid precipitation (pH 5, 30 °C) – Q-Sepharose FF] resulted in the same specific activity to within 0.5% (the yield of this alternative purification sequence was 33.6%).

Test for Co-Product: Hydrogen Peroxide or Water

Even though the literature and the sequences obtained from databases pointed towards water as the co-product of the reaction of both NADH oxidases, we embarked on a sensitive measurement of any putative hydrogen peroxide formed during NADH oxidase reaction. We utilized the horseradish peroxidase (HRP)-catalyzed oxidation of 9-acetylresorufin ("Amplex Red") to fluorescent resorufin as our assay. Amplex Red reacts with H_2O_2 according to a strict 1:1 stoichiometry

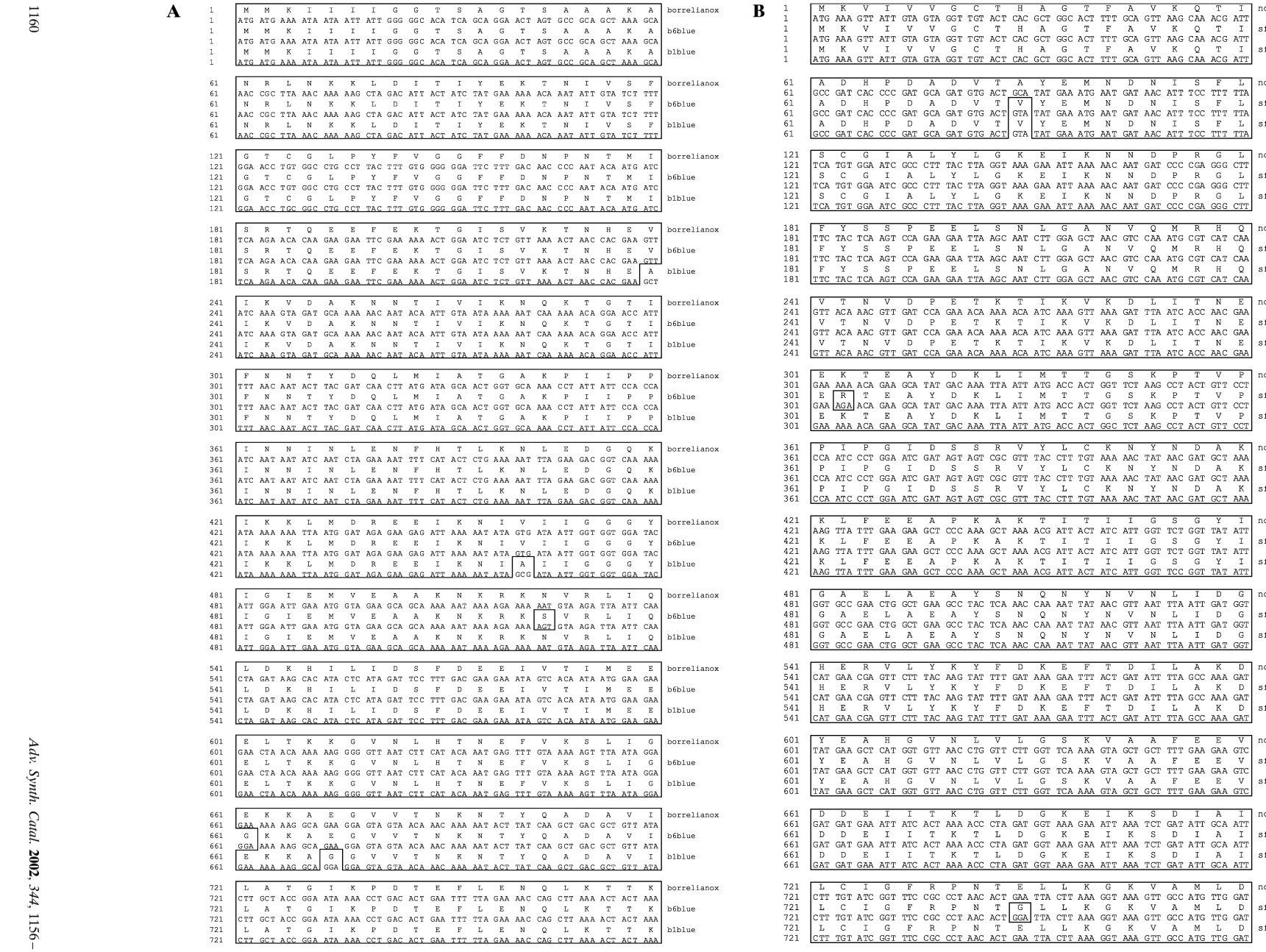
A
borrelianox
b6blue
b1blue
B
noxsanfran
sfk6seq
sfk2seq

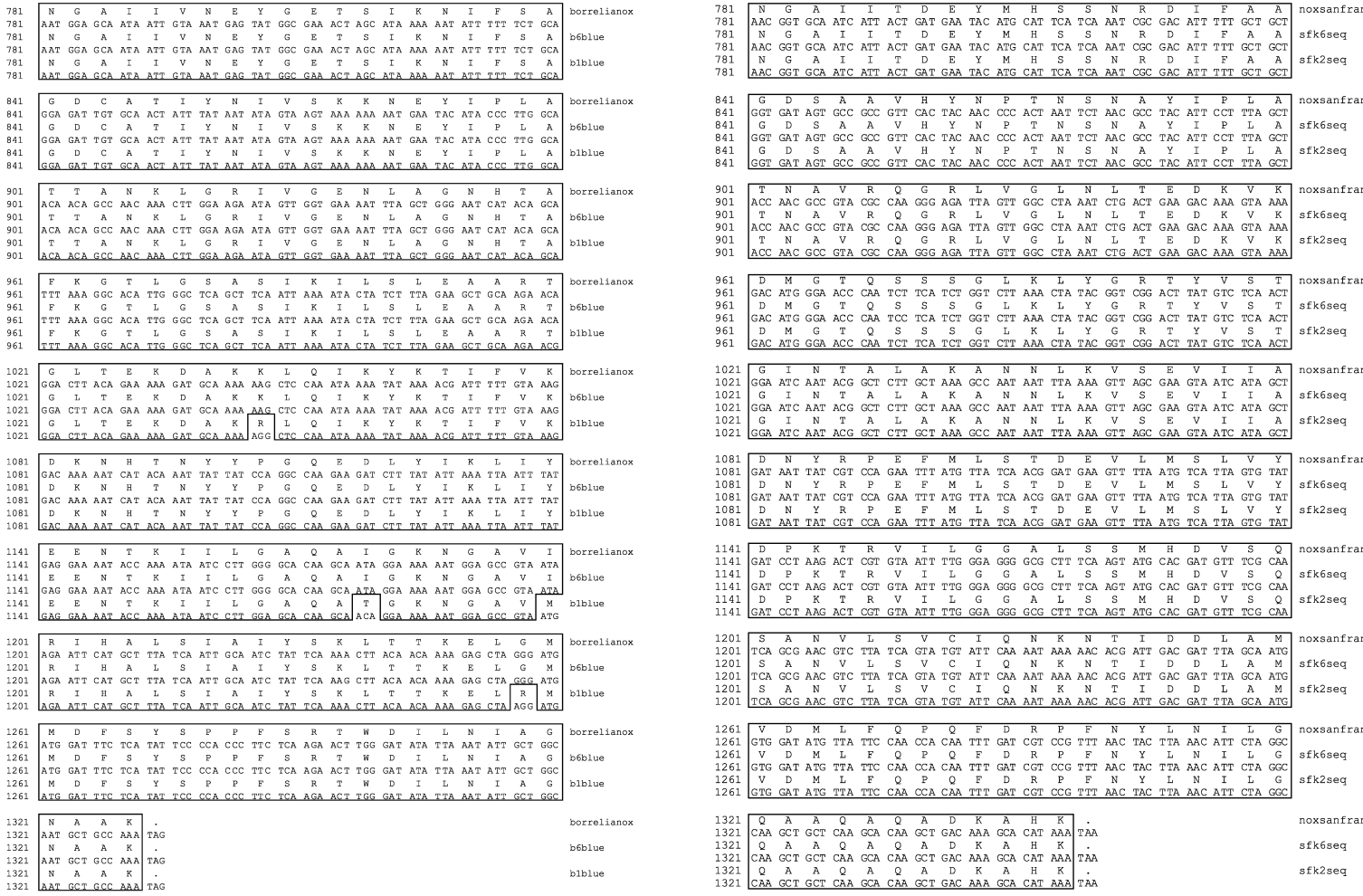

Figure 2. A: The complete nucleotide sequences of bnoxK1 and bnoxK6 as well as the respective deduced amino acid sequence are shown using a successfully expressed clone. The nucleotide sequence is compared to the annotated sequence available in the data bank. **B**: Parallel to part **A**, part **B** shows both nucleotide and deduced amino acid sequences of the sfnoxK2 and sfnoxK6 clones, similarly compared to the annotated nucleotide sequence in the data bank. The decoration box indicates an exact match to the annotated sequences.

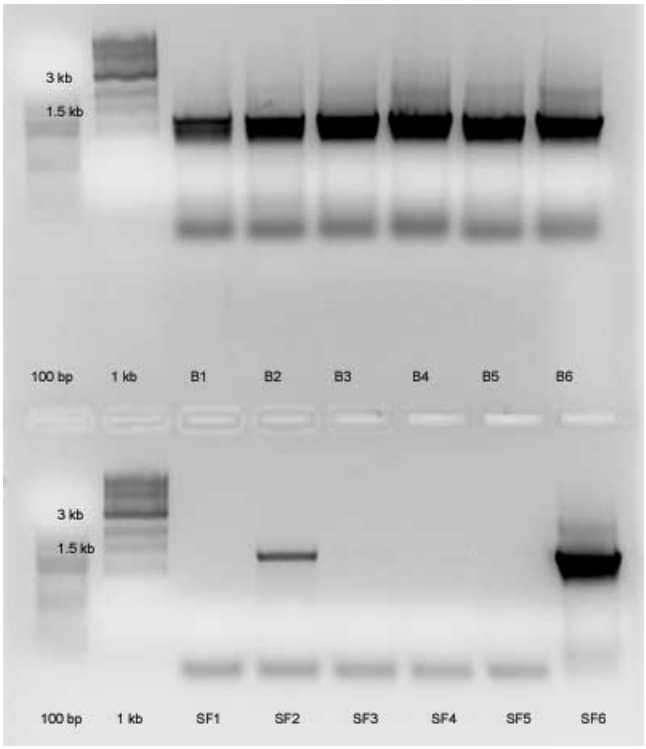

Figure 3. Colony PCR on five successfully transformed clones of bnox-pBTac2 and two of six tested positive for sfnox-pkk223-3. The bands in the figure show the amplified product of the expression plasmids after transformation. B1 – B6 demonstrate clones for bnox-pBTac2 and SF1 – 6 demonstrate clones for sfnox-pkk223-3.

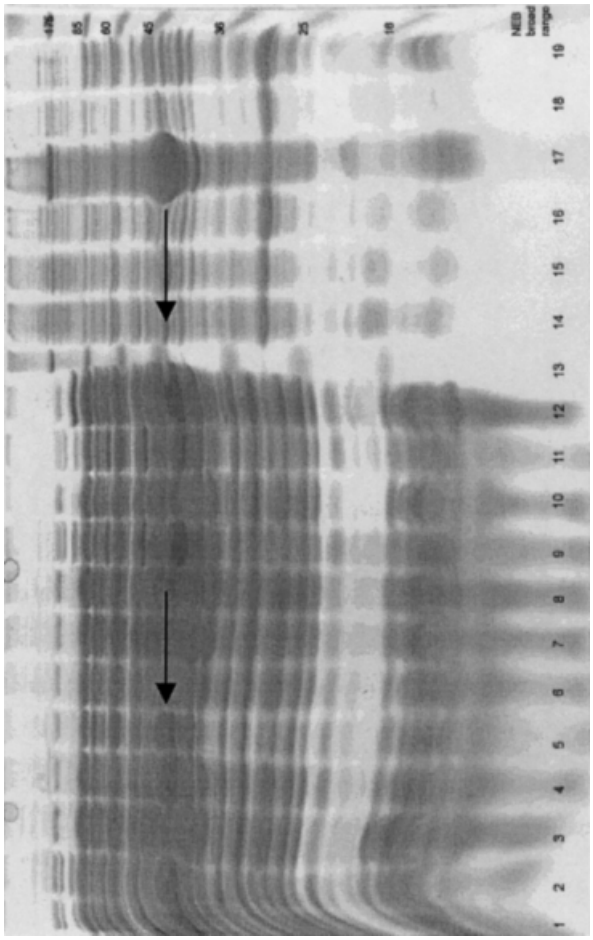

Figure 4. SDS-PAGE of insoluble and soluble fractions of sfnox K2 and K6 as well as bnoxK1 and K6. Lanes 1 – 12 represent the soluble fractions, lanes 14 – 19 the insoluble fractions. Lanes 1 – 4 show expression pattern of the sfnoxK2, lanes 1 and 3 are the uninduced fractions of 2 and 4, respectively. Lanes 3 and 4 show the sfnoxK2 with the additional helper plasmid pREP4. Lanes 5 and 6 represent sfnoxK6, with hardly any expression at all, but the corresponding insoluble fraction in lane 17 reveals overexpressed protein at 37 °C. Lanes 7 – 12 represent the bnox clones, 7 and 8 correspond to bnoxK1 and 9 – 12 to bnoxK6.

(Figure 6). The resorufin assay [λ_{max}: 587 nm (emission), $\varepsilon = 54{,}000$ L (mol cm)$^{-1}$] with its extremely low detection limit of 100 nM resorufin product is much more sensitive than other assays, such as ABTS or *o*-dianisidine.[39–41]

We detected 0.6 μM resorufin above background (and thus an equal concentration of H_2O_2 formed) upon conversion of 300 μM NADH with the *L. sanfranciscensis* enzyme (0.2% yield) but could not detect any resorufin above background in our experiment with the enzyme from *B. burgdorferi*. The value found for the *L. sanfranciscensis* enzyme is still above the detection limit of 0.25 μM[39] so it might indicate leakage of H_2O_2 which is formed during the operation of NADH oxidase. Nevertheless, any H_2O_2 formed only constitutes a very minor component of the product flux of NADH oxidase

Table 2. Purification table for sfnox resulting in scalability and high yield.

Step	Volume [mL]	Activity [U/mL]	Protein [mg/mL]	Specific Activity [U/mg]	Yield [%]	Purification Factor	Σ U
Lysate (pH 5.0)	10.2	424.4	14.3	29.7	100.0	1.0	4329.3
Dialysis (60 kDa MWCO)/Acid Precip pH 4.8	10.5	277.4	5.4	51.8	67.3	1.7	2912.7
Mono-Q	1.0	476.7	5.1	93.1	57.8*	3.1	476.7
45% ammonium sulfate dialysis	0.35	1114.1	8.4	132.6	47.3[a]	4.5	390.0

[a] Estimated theoretical yield for entire preparation.

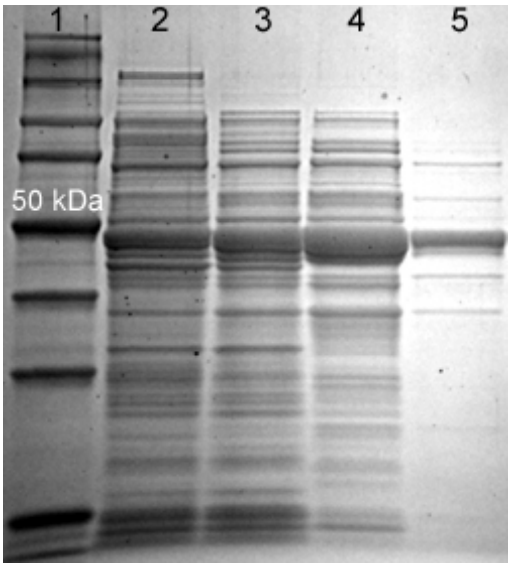

Figure 5. SDS-PAGE (12% Tris Glycine) corresponding to purification table a) Lane 1 is Prosieve® protein standards 5 to 225 kDa. The prominent purified band in lane 5 is at around 50 kDa.

from *L. sanfranciscensis*. We therefore conclude that water indeed is the co-product formed during the NADH oxidase reaction of *L. sanfranciscensis* and *B. burgdorferi*. Given that we find a cysteine residue in position 42, this finding is consistent with previous work.[30]

Kinetics with NADH and NADPH

Investigation of kinetic parameters with NADH and NADPH cofactors as substrates was performed with the supernatant of the 45% ammonium sulfate cut (40% for bnoxK6) in air-saturated solution at 30 °C and pH 7.0 in 0.1 M HEPES buffer. Figure 7 demonstrates that not only does the NADH oxidase of *L. sanfranciscensis* accept NADPH as a substrate with good reactivity ($v_{max} = 11$ U/mg), about 30% of activity towards NADH ($v_{max} = 39.3$ U/mg), but nearly identical K_M values of 6.7 and 6.1 μM indicate similar binding affinity. In contrast, the enzyme from *B. burgdorferi* only accepts NADH and at a higher K_M value of 22.0 μM than for the enzyme from *L. sanfranciscensis*. Chi values and error bars reveal high accuracy with $< 10\%$ error in most cases.

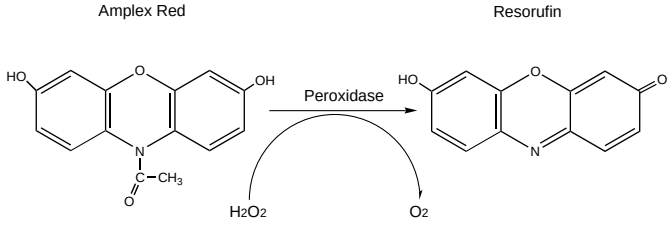

Figure 6. Assay for small amounts of hydrogen peroxide through HRP-catalyzed oxidation of Amplex Red to resorufin.

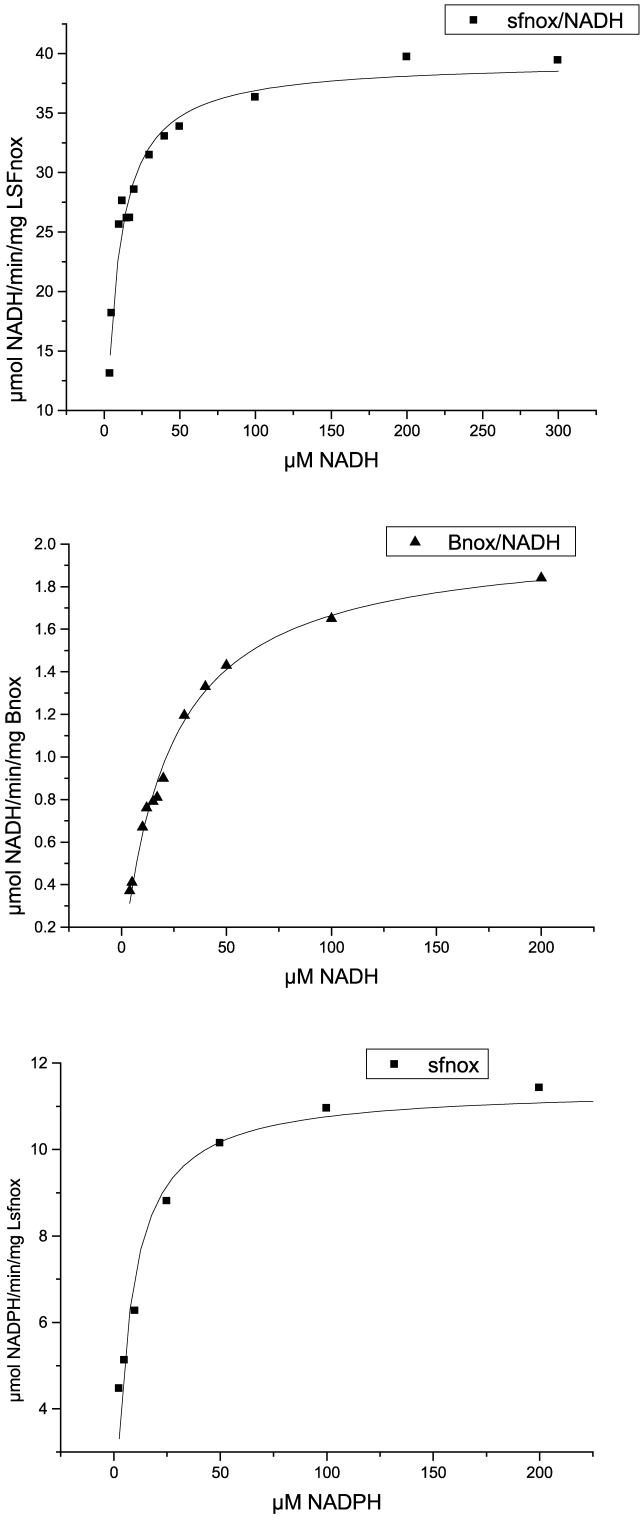

Figure 7. Kinetics of sfnox and bnox NADH oxidases with NAD(P)H cofactor in air-saturated solution at pH 7 and 30 °C.

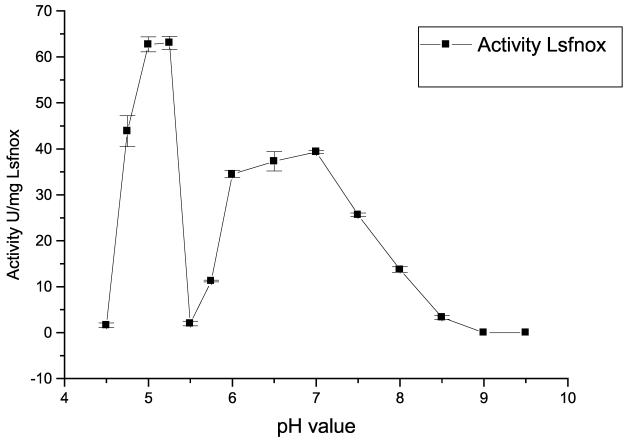

Figure 8. Activity-pH-profile of *L. sanfranciscensis* NADH oxidase.

Activity Profile with Respect to pH Value

With the supernatant of the 45% ammonium sulfate cut, an activity-pH profile was measured for the enzyme from *L. sanfranciscensis* (Figure 8). The pH optimum of activity was found at pH 5.2. Below pH 5, activity decreased markedly and reached zero at pH 4.5. Rates at pH 4.5 to 5.2 are reported as net rates, with the chemical decomposition rate at low pH subtracted. At pH values above 5.2, activity falls off sharply before recovering significantly at pH 6.0, reaching a peak at pH 7.0, and then gradually leveling off up to pH 8.5. The sharp activity decline between pH 5.2 and 6.0 coincides with the enzyme's pI, calculated to be pH 5.4. At pH 5.5, samples instantaneously lose activity, except for a very small residual activity. The cause of the pH gap in the activity profile is under further investigation.

Discussion and Conclusion

We have successfully applied the sequence comparison-based approach to find novel NADH oxidases that reduce oxygen directly to water. Fingerprints of the FAD-binding region and the NADH cofactor-binding site as well as search of the conserved cysteine residue, which seems to be responsible for directing the co-product flow towards water rather than hydrogen peroxide, seem to be sufficient clues for finding a water-forming NADH oxidase. The two novel enzymes only share a modest 32% sequence identity in between themselves and only 34% identity to the noxes of either *Enterococcus faecalis*[30] or *Streptococcus mutans*,[32] except for 55% between sfnox and *E. faecalis*. Given that rather low degree of similarity, the question of dependence of high activity and specificity between NADH *vs.* NADPH should be an interesting one for future work.

Regarding the discrepancies of the sequences in the databases with those found experimentally in this work, comparison with the known sequences from *Enterococcus faecalis* and *Streptococcus mutans* showing valine in position 30 in both cases suggests that our experimental result, V30, is correct rather than A30, the result in the sfnox database sequence (Accession file AB035801, NCBI). Bnox (accession file NC 001318, NCBI) is less identical to the known sequences than sfnox, so the relevance of the N175S and E221G changes is difficult to discern. As the specific activity of the *Borrelia* enzyme is considerably lower than that of the *Lactobacillus* protein, we will further investigate the influence of residues such as 175 or 221 using site specific mutagenesis.

A novel assay for H_2O_2, based on fluorescence of resorufin rather than on UV-VIS spectroscopy of ABTS or *o*-dianisidine, has been employed successfully to demonstrate that both NADH oxidases investigated here do indeed form H_2O instead of H_2O_2 as co-product. With its detection limit of 100 nM, the test based on 9-acetylresorufin ("Amplex Red") is much more sensitive than the other assays mentioned. While we have demonstrated that considerably more than 99.5% of the product flux ends up as water, we cannot yet exclude the possibility of a small shunt leading to H_2O_2. We will re-investigate this possibility with pure proteins under a variety of conditions to try to understand whether a consistent, albeit small, amount of H_2O_2 is formed during operation of one or both of the investigated NADH oxidases.

Regarding the kinetics of the enzyme from *L. sanfranciscensis*, it was found that both NADH and NADPH bind rather tightly, as judged by the low K_M value of 6.7 μM. Surprisingly, however, NADPH turned out to be almost as good a substrate as NADH: its v_{max} of 11 U/mg (at pH 7.0) is about a quarter of the value for NADH with 39.3 U/mg. This opens the potential for not just regenerating NAD^+ from NADH but also $NADP^+$ from NADPH. The enzyme from *L. sanfranciscensis* is much more active in comparison with the NADH oxidase from *B. burgdorferi*: at comparable degree of purity, the latter only has a v_{max} of 2.03 U/mg, and furthermore does not accept NADPH as a substrate.

The activity profile as a function of pH showed a surprising feature: instead of a bell-shaped curve we found a bimodal curve with a minimum around pH 5.5. As this pH value is very close to the calculated pI value of pH 5.4, we surmise that the enzyme is not active and/or not stable at its pI value (although the pI value has to be corroborated experimentally). As a pH optimum in the acidic range is not very common, the superposition of pH optimum and pI does not happen frequently. This phenomenon is under further investigation.

Experimental Section

Bacterial Strains, Media and Growth Conditions

The genomic DNA from *Borrelia burgdorferi* (ATCC 35210) and the strain *Lactobacillus sanfranciscensis* (ATCC 27651) were obtained from ATCC and grown in MRS medium (Gibco) at pH 6.5 under facultatively anaerobic conditions at 30 °C in quiescent culture. For expression of wild-type NADH oxidase, the *L. sanfranciscensis* strain was grown in the same medium, but under aeration with 120 rpm in an Infors shaker at 30 °C.

Host strains of *E. coli* were grown in Luria-Bertani medium at pH 7.5 and 37 °C, for cloning purposes or routine growth and plasmid production the host strain XL1 blue (Stratagene, La Jolla) was used. For expression purposes an HB101 strain (Stratagene, La Jolla) or M15 strain including the pREP4 plasmid (Qiagen, Hilden) was employed. These *E. coli* strains were grown at 30 °C under agitation for optimized expression levels. Ampicillin was added to the medium at a final concentration of 100 μg/mL to maintain selection pressure. To the M15 strain, 25 μg/mL kanamycin was added to maintain the additional helper plasmid.

Plasmids used: For cloning and sequencing, target genes were cloned into pBluescript (Stratagene, La Jolla); for expression either the pkk223-3 (Amersham) or pBTac2 (Roche) were chosen.

Manipulation and Amplification of DNA

The nox DNA sequences were identified using a search of the NCBI Genebank (Accession files AB035801 for *L. sanfranciscensis* nox and NC 001318 for *B. burgdorferi* nox). The corresponding specific 5′ and 3′ primers were synthesized at MWG Biotech (High Point, NC).

Primer optimization was performed using a primer design program (webbased design, http://genome-www2.stanford.edu/cgi-bin/SGD/web-primer). The nox genes from *L. sanfranciscensis* and *B. burgdorferi* were amplified using PCR and the gene-specific primers. Restriction sites used are underlined.

Primer Sequences

Amplification of the target DNA was performed using the protocol from the failsafe PCR kit (Epicentre, Madison). 12 reactions using 12 different buffers were set up and tested for optimal conditions. Setting up the PCR reactions involved final DNA concentration of 100 ng (*L. sanfranciscensis*) and 3.4 ng (*B. burgdorferi*), 200 μM of each dNTP, 10 μM of each primer and 1 U of Taq polymerase (Epicentre, Madison) in a final volume of 25 μL. To each of these reactions, 25 μL of each of the twelve doubly concentrated reaction buffer was added. DNA was amplified successfully for 30 cycles in an Eppendorf Gradient Thermocycler (Eppendorf, Hamburg) using the following conditions: each cycle involved a denaturing step at 30 sec 94 °C, an annealing step at 30 sec 60 °C or 68 °C, and an extension step at 2 min 72 °C. Of the final reaction mixture, 50 μL were analyzed on 1% agarose gels stained with 0.05% ethidium bromide. Prior to any further use, these PCR products were gel purified using the gel extraction kit (Qiagen, Hilden).

Cloning

Nox-specific DNA from *L. sanfranciscensis* was ligated into pBluescript (Stratagene, La Jolla) using EcoR1 (5′) and HindIII (3′) restriction sites and accordingly, nox from *B. burgdorferi* with BamH1(5′) and HindIII (3′) restriction sites. For all necessary ligations the Rapid Ligation kit protocol (Roche, Penzberg) was followed. The same pmol amounts of DNA were ligated, concentrations were calculated accordingly using the spectrophotometrically determined 260/280 nm ratio. Wild-type or mutant expression clones were constructed with the same restriction sites of Nox-*L. sanfranciscensis* (Lsfnox) into pkk223-3 (Amersham, Piscataway, NJ) and nox-*B. burgdorferi* (Bnox) into pBtac2 (Roche, Penzberg). Positive clones were tested either through colony PCR or restriction digest after plasmid preparation using the Miniprep Spin kit (Qiagen, Hilden).

Colony PCR

Colonies of the transformation plate were picked and first transferred onto a master plate, then suspended into 50 μl of lysis buffer containing Triton-X-100 (20 mM Tris pH 8.5 + 5 mM EDTA + 1% Triton X-100). After denaturing at 95 °C for 15 min, the solution was vortexed for 10 seconds and then 5 μL of the extract were tested in PCR (total volume 50 μL) using the gene specific primers.

Plasmid Preparation

5 mL LB_{amp} were inoculated with a colony and grown overnight at 37 °C. Cells were harvested by centrifugation (10000 rpm, 5 min, Eppendorf centrifuge, Hamburg) and plasmid DNA was isolated following the manufacturer's protocol (Miniprep Spin Kit, Qiagen, Hilden). Plasmid DNA was eluted into 50 μL water and 5 μL were digested with the corresponding restriction enzymes at the sites used for cloning and ligating.

N- and C-terminal primers for *L. sanfranciscensis*		
5′ gcg c gaattc atg aaa gtt att gta gta ggt tgt act	3′ sanfranseco	T_m 67.2 °C
5′ gcg c aagctt tta ttt atg tgc ttt gtc agc ttg tgc	3′ sanfranashind	T_m 62.8 °C
N- and C-terminal primers for *B. burgdorferi*		
5′ gcg c gg atc c at gat gaa aat aat aat tat tgg ggg	3′ borrnoxs	T_m 69.5 °C
5′ gcg c aa gct t ct att tgg cag cat tgc cag caa tat t	3′ borrnoxas	T_m 70.6 °C

Sequencing

20 μg of plasmid DNA (using the pBluescript vector) were sent off for sequencing using the same primers as for amplification in PCR. The templates were labeled with Applied Biosystems' "BigDye Terminator v3.0 Cycle Sequencing Ready Reaction" Kit for 25 cycles. Excess dye terminator molecules were removed with Qiagen Dye-Ex Spin Columns (Qiagen, Hilden). The samples were analyzed on the Applied Biosystems 3100 Genetic Analyzer (Perkin-Elmer-AB, Boston).

Expression of the nox Genes

Heterologous expression of the nox genes in *E. coli* was performed as follows: 5 mL starter LB_{amp} cultures were inoculated with aliquots from frozen stock cultures containing either bnox-pBTac2 or sfnox-pkk223-3 and grown overnight at 37 °C. These starter cultures were used to inoculate 200 mL cultures (1% v/v) or 1 L cultures (1% v/v), which were vigorously aerated until A_{600} reached 0.5 – 0.6, at which point the cultures were induced with 1 mM IPTG (final concentration) and protein expression was performed for 4 h. Cells were harvested and pellets frozen away at − 20 °C or used directly for enzyme activity assays.

For SDS-PAGE, 5 mL cultures were grown up to A_{600} of 0.5 and then induced with 1 mM IPTG for 4 h. Cells were harvested, resuspended in 200 μl TE50/50 (50 mM Tris, 50 mM EDTA pH 8.0), and sonicated for 2 × 15 sec with ice cooling. Supernatant (representing the soluble fraction) was separated after centrifugation and the insoluble fraction was resuspended in 200 μl TE 50/50 and shortly sonicated (5 sec) to dissolve the pellet. 10% SDS sample buffer was added (10% glycerol, 2% SDS, 0.063 M Tris/HCl pH 6.8, 0.1% bromophenol blue + either 10% β-mercaptoethanol or 75 mM DTT) and 30 μL analyzed on a 12.5% SDS-PAGE, stained with Coomassie blue (Pierce gel code staining solution, Pierce, Rockford, IL). Standard proteins used for molecular mass determination were obtained from New England Biolabs (Beverly, MA; broad range molecular weight markers, prestained).

Enzyme Assays

Nox activity assay: Cell-free extracts of the recombinant sfnox and bnox *E. coli* strains were prepared using ultrasonication described above in 0.1 M TEA pH 7.5 + 5 mM DTT or ß-mercaptoethanol. Nox activities were assayed at 30 °C in a total volume of 1 mL at 340 nm using the following conditions: in 0.1 M TEA pH 7.5 a final concentration of 0.2 mM NADH was dissolved and 10 μL enzyme solution were added. Enzyme reaction was followed for 1 min, activity was calculated using an extinction coefficient ε of NADH of 6.22 L/(mol cm).

Fermentation

Production strains were grown in 5 mL cultures at 37 °C and 250 rpm in 15 mL disposable culture tubes to 1.0 OD 600 nm in LB media + 100 μg/mL ampicillin. One liter cultures of LB medium supplemented with 5 g/L glycerol were seeded with 1 mL of the starter culture and grown at 30 °C and 200 rpm. Both baffled and unbaffled Fernbach shake flasks were used for fermentation. When the cultures reached 1.0 OD 600 nm the flasks were induced by addition of 0.5 mM IPTG and grown for an additional 3 – 4 hours. Additional ampicillin, 200 μg/ml, was added at induction and every hour thereafter to maintain selection pressure on the culture. When helper plasmids were present in the strains 50 μg/mL kanamycin was also added to the culture. Cultures were harvested by centrifugation at 5000 rpm in 1 L centrifuge containers (Beckman J2-M) and the resulting cell pellet was frozen at − 80 °C.

Purification of sfnoxK2 Enzyme

Frozen cell pellets were thawed and resuspended in 10 mL of 100 mM potassium phosphate buffer pH 6.8 + 1 mM EDTA + 5 mM DTT + 5 mM spermine. The cell slurry was then sonicated with a Fisher Scientific 60 Sonic dismembrator for 6 × 2 minutes while floating the tube in ice/water for cooling. The resulting lysate was centrifuged at 18,000 rpm in a Beckman J2-21M for 45 minutes at 4 °C. The clarified lysate was then loaded into Spectro/Por® regenerated cellulose dialysis membrane tubing (60 K MWCO) and dialyzed against 1 L of 45% ammonium sulfate + 50 mM potassium phosphate buffer pH 6.8 + 1 mM EDTA + 5 mM DTT. After four hours the sample was transferred to a second freshly prepared 45% ammonium sulfate solution. Following an additional 8 hours of dialysis (overnight), the sample was centrifuged at 18,000 rpm for 15 minutes at 4 °C. The resulting solution was transferred to a Pierce Slide-A-Lyzer® dialysis cassette (10 K MWCO) and dialyzed versus 20 mM 1-methylpiperazine buffer pH 5.0 and 30 °C + 5 mM DTT. The sample was dialyzed versus a liter of buffer for two hours at 30 °C with stirring (200 rpm) on a digital magnetic stirplate/heater with a temperature probe to maintain the solution at 30 °C. A buffer exchange was performed after one hour of dialysis. The sample was then transferred and centrifuged at 18,000 rpm for 15 minutes at 4 °C. The resulting solution was then loaded onto a Amersham Pharmacia HiPrep 16/10 Q FF column on an AKTA system at 4 °C. A gradient separation was performed from 0 to 100% 1 M NaCl with the running buffer 20 mM 1-methylpiperazine buffer pH 5.0 at 4 °C. 5 mL fractions were collected over the course of the run and the nine most active fractions were pooled.

A second purification protocol utilized 100 mM 1-methylpiperazine buffer pH 5.0 in the lysis buffer. Frozen cell pellets were thawed and resuspended in 10 mL of 100 mM 1-methylpiperazine buffer pH 5.0 + 1 mM EDTA + 5 mM DTT + 5 mM spermine. The cell slurry was then sonicated with a Fisher Scientific 60 Sonic dismembrator for 6 × 2 minutes while floating the tube in ice/water for cooling. The resulting lysate was centrifuged at 18,000 rpm in a Beckman J2-21M for 45 minutes at 4 °C. The clarified lysate was then loaded into Spectro/Por® regenerated cellulose dialysis membrane tubing (60 K MWCO) and dialyzed with 1 L of 20 mM 1-methylpiperazine buffer pH 5.0 at 35 °C + 5 mM DTT. The sample was dialyzed versus 1 L of buffer for two hours at 35 °C with stirring (200 rpm) on a digital magnetic stirplate/heater with a temperature probe to maintain the solution at 35 °C. A buffer exchange was performed after one hour of dialysis. The sample was then transferred and centrifuged at 18,000 rpm for 15 minutes at 4 °C. The resulting solution was then loaded onto a Amersham Pharmacia Mono-Q column on an AKTA system at 4 °C. A gradient separation over 10 column volumes was

performed from 0 to 100% 1 M NaCl with the running buffer 20 mM 1-methylpiperazine buffer pH 5.0 at 4 °C. 1 mL fractions were collected over the course of the run and the most active fraction was dialyzed *versus* 45% ammonium sulfate + 50 mM potassium phosphate buffer pH 6.2 + 1 mM EDTA + 5 mM DTT. After four hours the sample was transferred to a second freshly prepared 1.5 L of 45% ammonium sulfate solution. Following an additional 4 hours of dialysis the sample was centrifuged at 18,000 rpm for 15 minutes at 4 °C.

Hydrogen Peroxide Assay

For the sensitive assay of putative hydrogen peroxide formation during the reaction of NADH oxidase the horseradish peroxidase-catalyzed oxidation of 9-acetylresorufin was employed. The Amplex Red hydrogen peroxide assay kit (A-22188) from molecular probes was utilized for these assays. Following the protocols outlined in the kit instructions, a standard curve of H_2O_2 was prepared in the reaction buffer (50 mM sodium phosphate buffer pH 7.4) from the peroxide stock. The prepared concentrations were 20, 10, 5, and 2.5 μM H_2O_2 and 0 as a control. A working solution of 100 μM Amplex Red reagent and 0.2 U/ml horseradish peroxidase (HRP) was prepared in the reaction buffer as per kit instructions. As NADH and other reducing reagents are known to interfere with the Amplex Red assay, the NADH oxidase enzymes were allowed to react with the substrate immediately prior to the Amplex Red analysis. Reaction buffer from the kit was utilized in running enzyme test with 300 μM NADH as well as the controls without NADH. The enzyme conversions were performed by adding 3 μL of enzyme prep to 3 mL of reaction buffer with 300 μM NADH, mixing, and following the conversion until completion by absorbance at 340 nm. 50 μL of the final reaction mixture and standard curve solutions were added to each well in a 96-well fluorescence plate (costar, black, pp). Five replicates were made per sample and standard curve point. 50 μL of the Amplex Red reagent were added to each well and incubated for 30 minutes at 30 °C. Fluorescence readings were performed in a BMG FLUOstar Galaxy microplate reader with 544ex/590em filter settings.

Kinetics of Cofactor Substrates

The kinetic analysis was performed on ammonium sulfate fractions from both the sfnox and bnox strains in 50 mM HEPES buffer pH 7.0 at 30 °C. The initial enzyme fractions were diluted in 25 mM HEPES pH 7.0 at 30 °C + 25% glycerol + 5 mM DTT to approximately − 0.05 A340 nm/min and retained on ice during analysis. Conversion of NAD(P)H was followed by change of absorbance at 340 nm in a Jasco V-530 spectrophotometer. 3 mL methyl acrylate disposable cuvettes were used for all experiments and all runs were performed in triplicate at 30 °C. Reactions with NADH were started by adding 3 μL of enzyme preparation, 9 μL for NADPH, to the cuvette and mixing by inversion with parafilm three times. Varying concentrations of NAD(P)H substrate were made by preparing 100 mL of a 300 μM solution in a volumetric flask. Dilutions of this solution were then made to provide the differing substrate concentrations for the kinetic profile.

Activity-pH Profile of sfnoxK2

The pH profile was performed on ammonium sulfate fractions from the sfnoxK2. 100 mM buffer solutions at 30 °C and 200 μM NADH were used for activity analysis as monitored by absorbance at 340 nm. All samples were tested in triplicate in 3 mL methyl acrylate disposable cuvettes. The following buffers were utilized within the buffering range of 1 pH unit from their pKa: acetate, *N*-methylpiperazine, MES (2-[*N*-morpholino]ethanesulfonic acid hydrate), and bis-tris-propane. Sodium hydroxide or hydrochloric acid were used in preparation of the respective buffers.

Protein Gel Analysis

Prior to SDS-PAGE, protein samples were diluted to 2 mg/mL concentration in deionized water if the initial concentration was above 2 mg/mL. The 50 μL diluted samples were then mixed with 50 μL of 2X sample buffer composed of 125 mM Tris-HCl, pH 6.8, 4% SDS, 50% glycerol, 0.02% bromophenol blue, and 10% 2-mercaptoethanol. Mixed samples were incubated at 100 °C for 5 minutes and then placed on ice. 10 to 20 μL of the samples were loaded onto a 12% PAGEr™ Gold precast gel and run in a Hoefer SE260 chamber at 125 V for 2 hours (running buffer: 25 mM Tris base, 192 mM glycine, 0.1% SDS) with chilling water circulating at 4 °C. Molecular weight standards ProSieve® from BMA or Precision Plus Protein™ standards from Bio-Rad were added to lanes immediately adjacent to the sample lanes.

Determination of Protein Concentration

Protein concentration was determined by the Bradford method utilizing Coomassie Plus Protein assay reagent and pre-diluted protein assay standards-BSA (Pierce Chemical) for the calibration curve. Coomassie blue from Pierce (gelcode blue stain reagent, Pierce, Rockford, IL) were used in staining.

References

[1] A. Zaks, *Curr. Opin. Chem. Biol*. **2001**, *5*, 130 – 136.
[2] A. Liese, M. V. Filho, *Curr. Opin. Biotechnol*. **1999**, 10, 595 – 603.
[3] J. D. Rozzell, *Chimica Oggi* **1999**, 42 – 47.
[4] A. S. Bommarius, M. Schwarm, K. Drauz, *Chimia* **2001**, *55*, 50 – 59.
[5] D. A. Evans, T. C. Britton, J. A. Ellman, R. L. Dorow, *J. Am. Chem. Soc.* **1990**, *112*, 4011 – 4030.
[6] U. Groth, C. Schmeck, U. Schöllkopf, *Liebigs Ann. Chem*. **1993**, 321-323.
[7] W. Hummel, *Adv. Biochem. Eng. Biotechnol*. **1997**, *58*, 145 – 184.
[8] M. J. Kim, G. M. Whitesides, *J. Am. Chem. Soc*. **1988**, *110*, 2959 – 2964.
[9] H. K. W. Kallwass, *Enzyme Microb. Technol*. **1992**, *14*, 28 – 35.
[10] G. Krix, A. S. Bommarius, K. Drauz, M. Kottenhahn, M. Schwarm, M.-R. Kula, *J. Biotechnology* **1997**, *53*, 29 – 39.

[11] Y. Asano, A. Yamada, Y. Kato, K. Yamaguchi, Y. Hibino, K. Hirai, K. Kondo, *J. Org. Chem.* **1990**, *55*, 5567 – 5571.
[12] C. W. Bradshaw, C. H. Wong, W. Hummel, M.-R. Kula, *Biorg. Chem.* **1991**, *19*, 29 – 39.
[13] R. L. Hanson, J. M. Howell, T. L. LaPorte, M. J. Donovan, D. L. Cazzulino, V. V. Zannella, M. A. Montana, V. B. Nanduri, S. R. Schwarz, R. F. Eiring, S. C. Durand, J. M. Wasylyk, W. L. Parker, M. S. Liu, F. J. Okuniewicz, B. Chen, J. C. Harris, K. J. Natalie, K. Ramig, S. Swaminathan, V. W. Rosso, S. K. Pack, B. T. Lotz, P. J. Bernot, A. Rusowicz, D. A. Lust, K. S. Tse, J. J. Venit, L. J. Szarka, R. N. Patel, *Enzyme Microb Technol* **2000**, *26*, 348 – 358.
[14] R. L. Hanson, M. D. S. A. Banerjee, D. B. Brzozowski, B.-C. Chen, B. P. Patel, C. G. McNamee, G. A. Kodersha, D. R. Kronenthal, R. N. Patel, L. J. Szarka, *Bioorganic & Medicinal Chemistry* **1999**, *7*, 2247 – 2252.
[15] A. Willetts, *Trends Biotechnol.* **1997**, *15*, 55 – 62.
[16] M.-R. Kula, *Enzyme catalyzed reductions of carbonyl groups*, Chiral Europe, Nice, France, Spring lnnovations, Ltd., Stockport UK, **1994**.
[17] W. Hummel, M.-R. Kula, *Eur. J. Biochem.* **1989**, *184*, 1 – 13.
[18] T. Ohshima, K. Soda, *Adv. Biochem. Eng./Biotech.* **1990**, *42*, 187 – 209.
[19] W. Hummel, *TIBTECH* **1999**, *17*, 487 – 492.
[20] R. Wichmann, C. Wandrey, A. F. Bückmann, M.-R. Kula, *Biotechnol. Bioeng.* **1981**, *23*, 2789 – 2802.
[21] M.-R. Kula, C. Wandrey, *Meth. Enzymol.* **1987**, *136*, 9 – 21.
[22] G. L. Lemière, J. A. Lepoivre, F. C. Alderweireldt, *Tetrahedron Lett.* **1985**, *26*, 4527 – 4528.
[23] a) M. D. Bednarski, H. K. Chenault, E. S. Simon, G. M. Whitesides, *J. Am. Chem. Soc.* **1987**, *109*, 1283 – 1285; b) H. K. Chenault, G. M. Whitesides, *Bioorg. Chem.* **1989**, 17, 400 – 409.
[24] G. Carrea, R. Bovara, R. Longhi, S. Riva, *Enz. Microb. Technol.* **1985**, *7*, 597 – 600.
[25] L. G. Lee, G. M. Whitesides, *J. Am. Chem. Soc.* **1985**, *107*, 6999 – 7008.
[26] H. J. Park, C. O. Reiser, S. Kondruweit, H. Erdmann, R. D. Schmid, M. Sprinzl, *Eur. J. Biochem.* **1992**, *205*, 881 – 885.
[27] R. E. Altomare, J. Kohler, P. F. Greenfield, J. R. Kittrell, *Biotechnol. Bioeng.* **1974**, *16*, 1659 – 1673.
[28] K. Koike, T. Kobayashi, S. Ito, M. Saitoh, *J. Biochem.* **1985**, *97*, 1279 – 1288.
[29] R. P. Ross, A. Claiborne, *J. Mol. Biol.* **1991**, *221*, 857 – 871.
[30] R. P. Ross, A. Claiborne, *J. Mol. Biol.* **1992**, *227*, 658 – 671.
[31] S. N. Peterson, P. C. Hu, K. F. Bott, C. A. Hutchinson 3rd, *J. Bacteriol.* **1993**, *175*, 7918 – 7930.
[32] J. Matsumoto, M. Higushi, M. Shimada, Y. Yamamoto, Y. Kamio, *Biosci. Biotech. Biochem.* **1996**, *60*, 39 – 43.
[33] C. J. Bult, O. White, G. J. Olsen, L. Zhou, R. D. Fleischmann, G. G. Sutton, J. A. Blake, L. M. FitzGerald, R. A. Clayton, J. D. Gocayne, A. R. Kerlavage, B. A. Dougherty, J. F. Tomb, M. D. Adams, C. I. Reich, R. Overbeek, E. F. Kirkness, K. G. Weinstock, J. M. Merrick, A. Glodek, J. L. Scott, N. S. Geoghagen, J. C. Venter, *Science* **1996**, *273*, 1058 – 1073.
[34] S. S. Mande, D. Parsonage, A. Claiborne, W. G. Hol, *Biochemistry* **1995**, *34*, 6985 – 6992.
[35] J. I. Yeh, A. Claiborne, W. G. Hol, *Biochemistry* **1996**, *35*, 9951 – 9957.
[36] T. Stehle, A. Claiborne, G. E. Schulz, *Eur. J. Biochem.* **1993**, *211*, 221 – 226.
[37] T. C. Mallett, A. Claiborne, *Biochemistry* **1998**, *37*, 8790 – 8802.
[38] R. K. Scopes, *Protein purification: principles and practice*, Springer, New York, 3rd edition, **1994**.
[39] S. Lindsay, D. Brosnahan, G. D. Watt, *Biochemistry* **2001**, *40*, 3340 – 3347.
[40] M. Zhou, Z. Diwu, N. Panchuk-Voloshina, R. P. Haugland, *Anal. Biochem.* **1997**, *253*, 162 – 168.
[41] J. G. Mohanty, J. S. Jaffe, E. S. Schulman, D. G. Raible, *J. Immunol. Methods* **1997**, *202*, 133 – 141.